# Supporting Information

# Triazine-Functionalized Covalent Benzoxazine Framework for Directly Synthesis of N-doped Microporous Carbon

**Hesham R. Abuzeid,[a] Ahmed F. M. EL-Mahdy,[a,b] Mahmoud M. M. Ahmed[a] and Shiao-Wei Kuo[a,c*]**

[a]Department of Materials and Optoelectronic Science, Center of Crystal Research, National Sun Yat-Sen University, Kaohsiung 80424, Taiwan, E-mail: kuosw@faculty.nsysu.edu.tw

[b]Chemistry Department, Faculty of Science, Assiut University, Assiut 71516, Egypt.

[c]Department of Medicinal and Applied Chemistry, Kaohsiung Medical University, Kaohsiung, 807, Taiwan

## Characterization

The NMR spectra of TAPT and THPT were measured using an INOVA 500 instrument with DMSO-$d_6$ as the solvent. Solid-state $^{13}C$ NMR spectra were recorded at room temperature using a Bruker DSX-400 spectrometer, based on the cross-polarization pulse sequence, broad band proton decoupling, and a magic-angle spinning (MAS) rate of 5.4 kHz to decrease the peak broadening. FTIR spectra of benzoxazine derivative were recorded using a Bruker Tensor 27 spectrophotometer. All samples were prepared using the typical KBr disk method; 32 scans were recorded at a spectral resolution of 1 $cm^{-1}$. The dynamic thermal curing behavior of BZ prepolymers was examined using a TA Q-20 DSC apparatus operated at a heating rate of 10 °C $min^{-1}$ from 25 to 400 °C under a $N_2$ atmosphere. The thermal stabilities and char yields of all the BZ prepolymers were measured using a TA Q-50 TGA apparatus; a heating rate of 10 °C $min^{-1}$ was applied from 25 to 800 °C under a $N_2$ atmosphere. Raman spectra were recorded using a Horiba Jobin-Yvon HR800 Raman spectrometer equipped with a 633-nm laser; 10-s accumulated scans were repeated 20 times; a 50x magnification lens was employed. XPS was performed using the Mg Kα radiation from the double anode at 50 W; the related binding energies of the samples in the high-resolution spectra were calibrated using the C 1s binding energy at 284.6 eV. X-ray diffraction patterns of BZ derivatives were recorded by the BL17A1 wiggler beam-line at the National Synchrotron Radiation Research Center (NSRRC), Taiwan; the wavelength (λ) was 1.24 Å. The $N_2$ adsorption/desorption and $CO_2$ adsorption isotherms were recorded using an ASAP 2020 analyzer. The N-doped microporous carbon was degassed at 150 °C for 2 h prior to measurement. The surface areas and pore volumes from the adsorption branches of the isotherms were measured using the BET method. The electrochemical performances were determined using a Zahner Zennium E electrochemical workstation in a three-electrode configuration, with Ag/AgCl as the reference electrode and 1.0 M KCl as the aqueous medium. The working electrode was an ITO substrate coated with the slurry of the tested material.[S1] CV was performed over the range from –1.0 to +1.0 V; scan rates were investigated from 5 to 200 mV $s^{-1}$. The

charge/discharge (CD) cycles were tested over the same potential range various current densities from 1 to 10 A $g^{-1}$. The capacitances (*C*) were calculated using the reported equations for CV and CD, respectively.[S2]

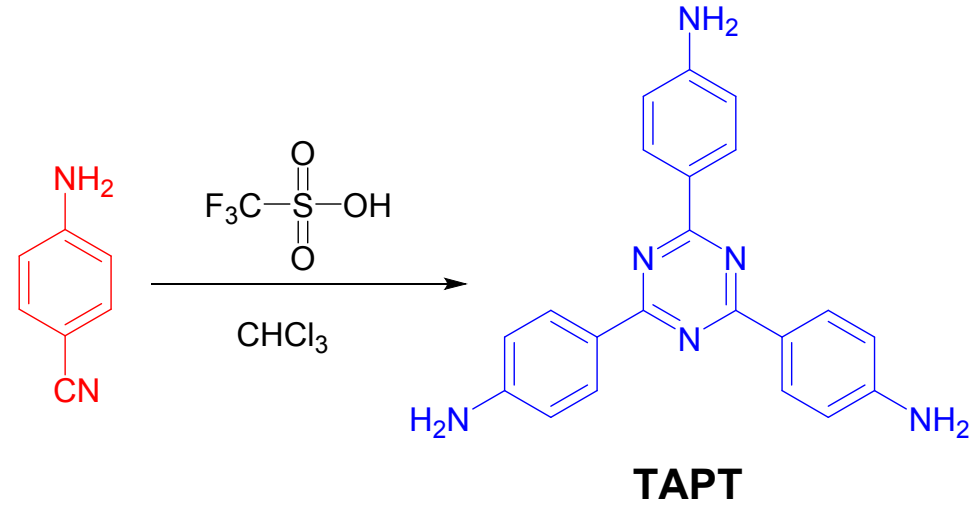


**Scheme S1.** Synthesis of 1,3,5-tris-(4-aminophenyl)triazine (TAPT)

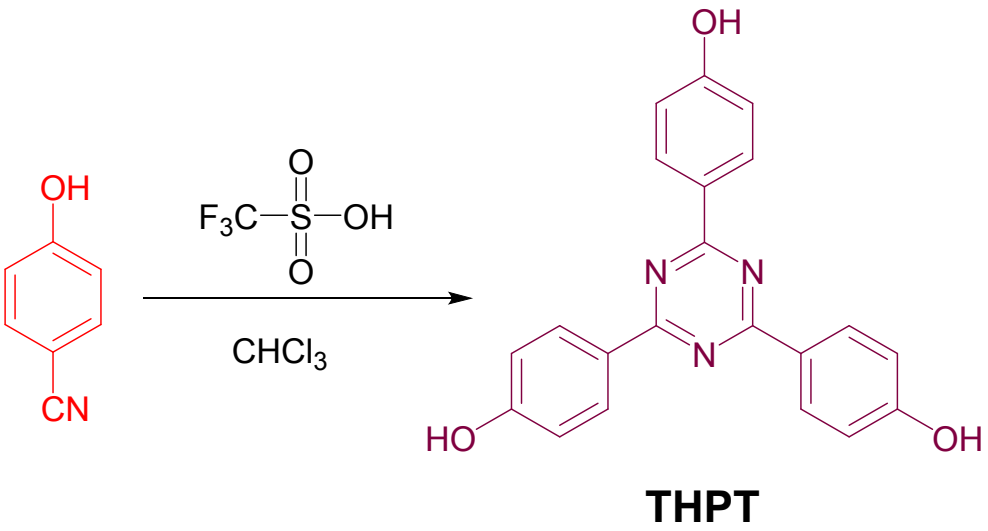


**Scheme S2.** Synthesis of 2,4,6-tris(4-hydroxyphenyl)triazine (THPT)

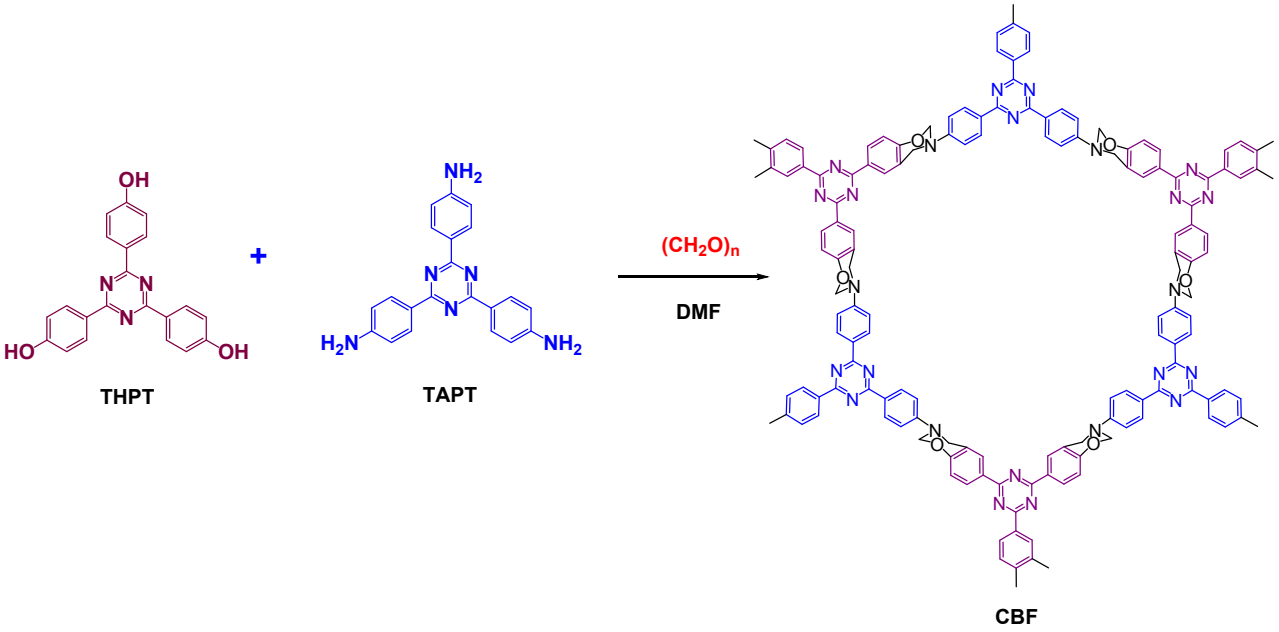


**Scheme S3.** Synthesis of covalent benzoxazine framework (**CBF**)

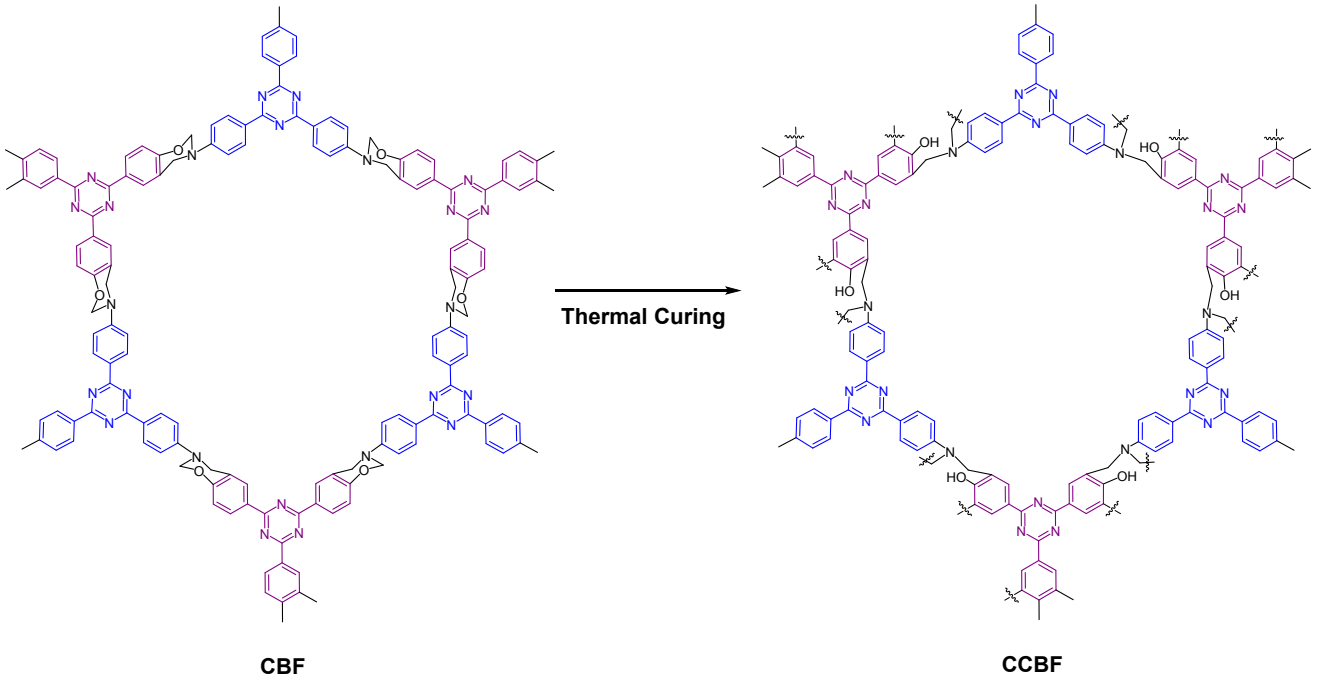


**Scheme S4.** Synthesis of cross-linked covalent triazine framework **(CCBF)**

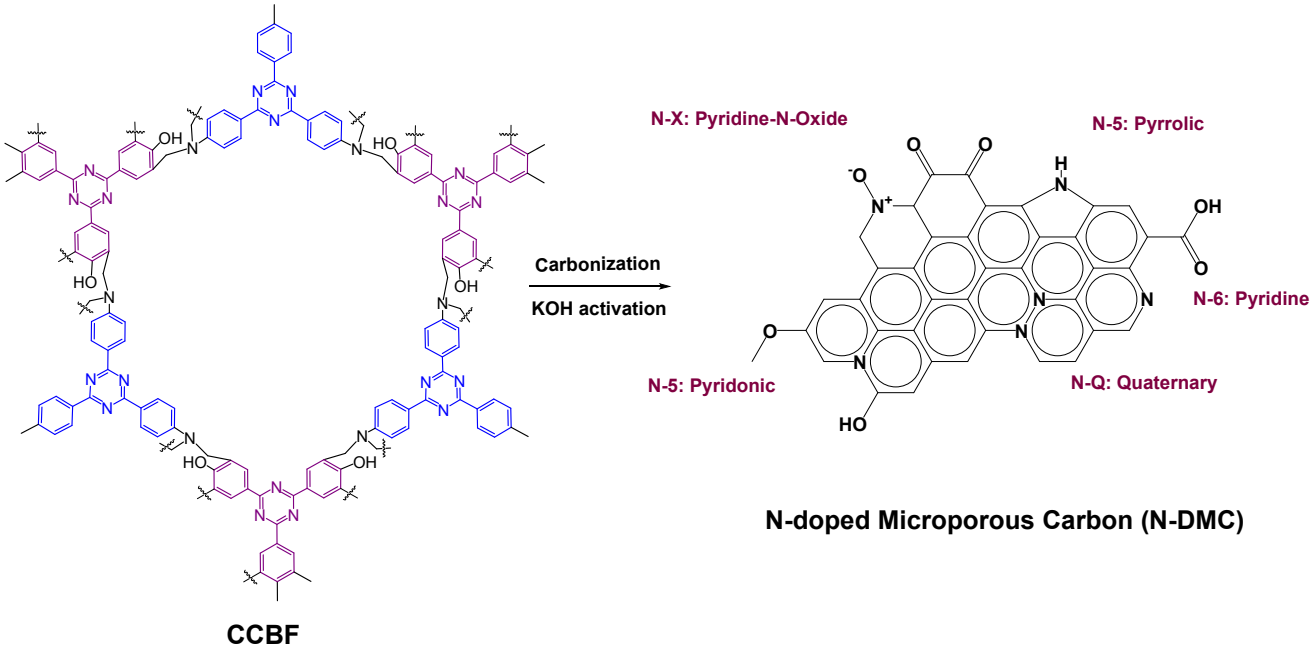


**Scheme S5.** Synthesis of N-doped microporous carbon **(N-DMC).**

**X-Ray Analysis**

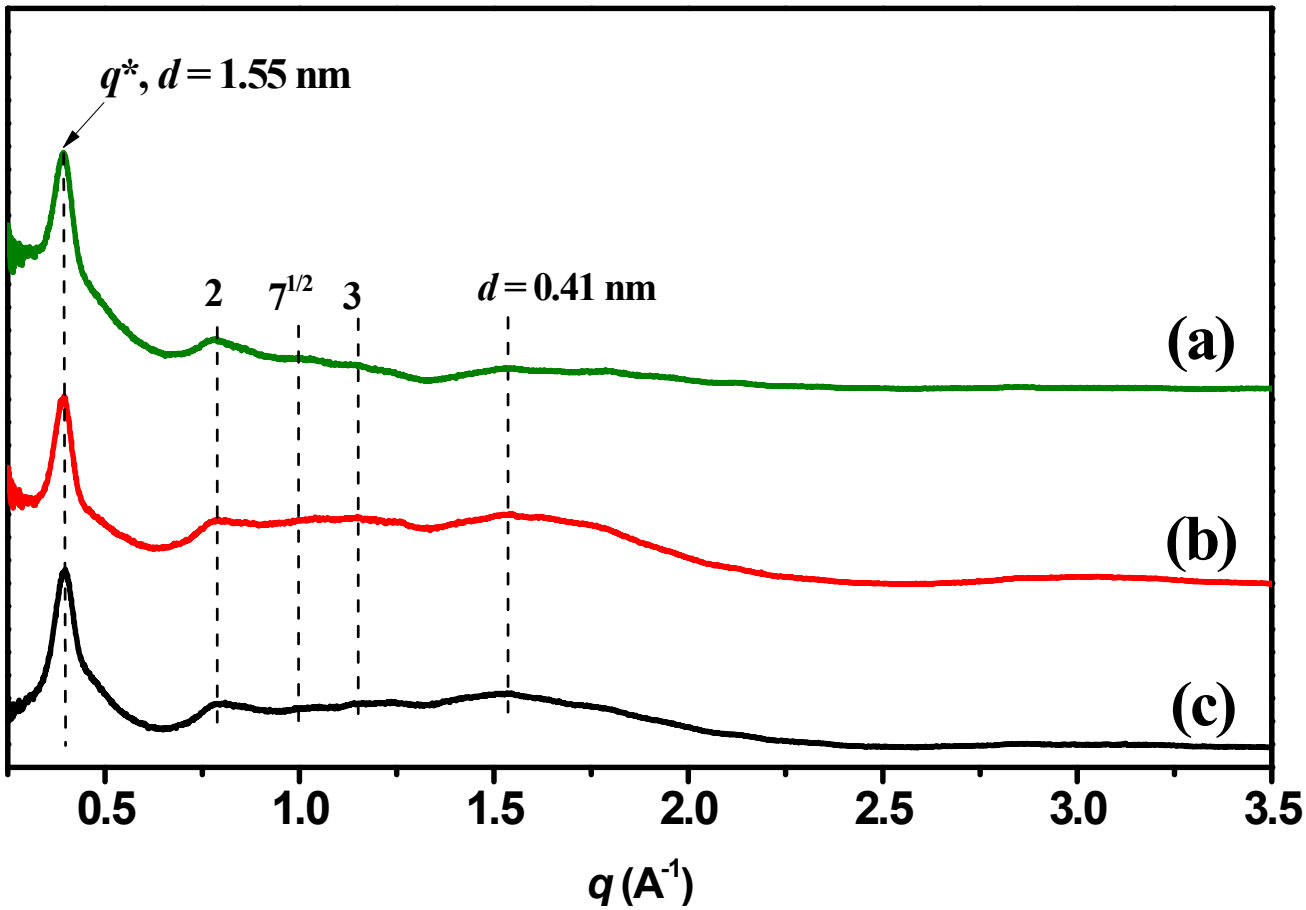


**Figure S1.** WAXD patterns of (a) CBF, (b) CCBF and (c) N-DMC.

**Structural Modeling of Covalent Benzoxazine Framework**

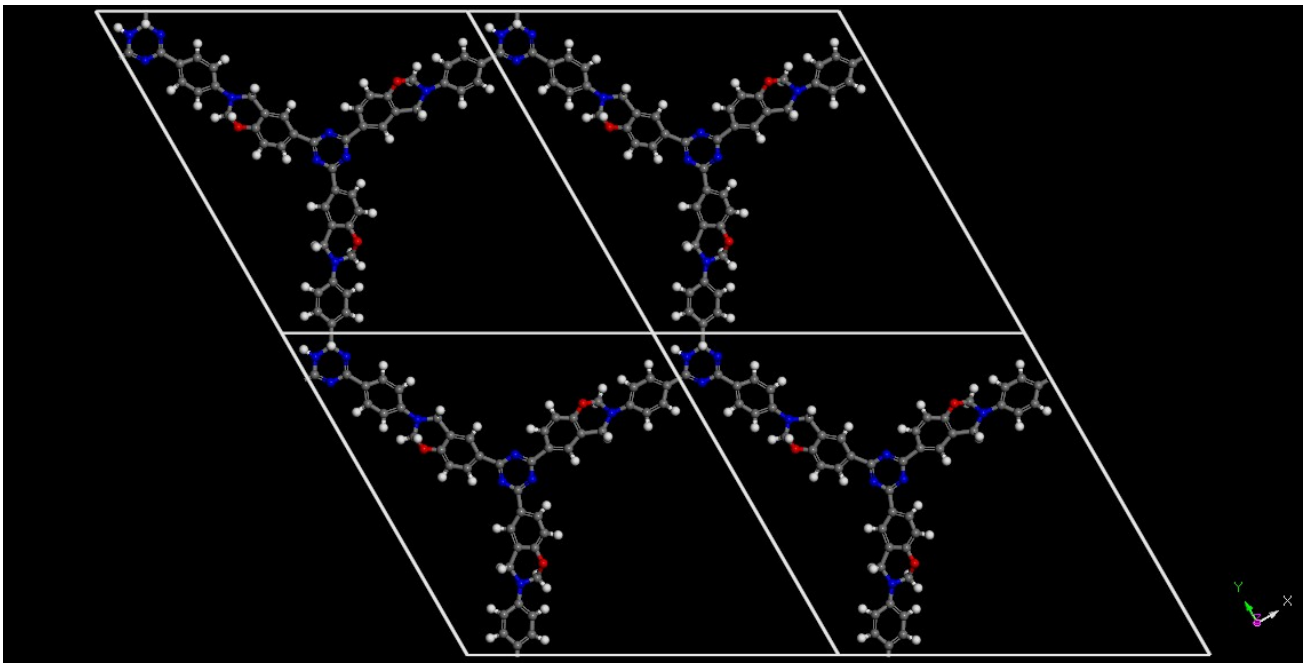

**Figure S2.** 3D-view of the simulated structure of the CBF along the *c* axis.

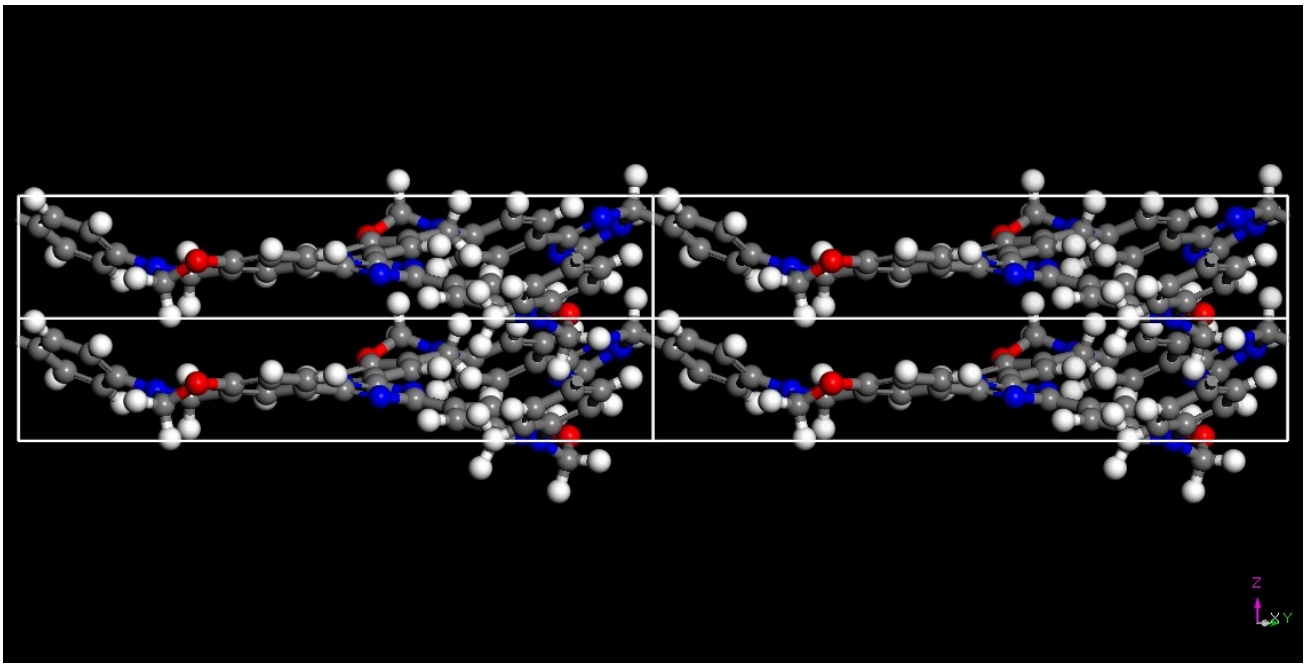

**Figure S3.** 3D-view of the simulated structure of the CBF along the *a* axis.

**Fractional atomic coordinates for Covalent Benzoxazine Framework Structure**

**Table S1.** Fractional atomic coordinates for the unit cell of CBF with AA-stacking.

| Sample name: CBF | | | | | | | |
|---|---|---|---|---|---|---|---|
| Space group: P1 | | | | | | | |
| a = 37.1498 Å, b = 26.7614 Å, c = 4.5896 Å, $\alpha = \beta = 90^\circ$, $\gamma = 120^\circ$ | | | | | | | |
| $R_{wp}$ = 13.51 %, $R_p$ = 9.69 % | | | | | | | |
| Atom | *x/a* | *y/b* | *z/c* | Atom | *x/a* | *y/b* | *z/c* |
| O1 | 0.11233 | 0.54023 | 0.77532 | C19 | 0.17757 | 0.49135 | 0.60996 |
| O2 | 0.69946 | 0.87881 | 0.15105 | C20 | 0.23799 | 0.49647 | 0.53402 |
| O3 | 0.43845 | 0.27792 | 0.23967 | C21 | 0.59106 | 0.69648 | 0.19896 |
| N4 | 0.36333 | 0.50713 | 0.42499 | C22 | 0.64706 | 0.75781 | 0.14633 |
| N5 | 0.47631 | 0.57131 | 0.31681 | C23 | 0.64409 | 0.81601 | 0.19584 |
| N6 | 0.41425 | 0.62247 | 0.43343 | C24 | 0.58515 | 0.81143 | 0.3059 |
| N7 | 0.76405 | 0.82857 | 0.05409 | C25 | 0.52931 | 0.74991 | 0.35845 |
| N8 | 0.16237 | 0.65577 | 0.86008 | C26 | 0.43337 | 0.33515 | 0.25395 |
| N9 | 0.32256 | 0.21359 | 0.20416 | C27 | 0.48999 | 0.39581 | 0.31471 |
| N10 | -1.94075 | 3.95174 | 1.69984 | C28 | 0.29587 | 0.55757 | 0.55302 |
| N11 | -1.96536 | 3.84316 | 1.6046 | C29 | 0.53183 | 0.69203 | 0.30469 |
| N12 | -1.86199 | 3.92015 | 1.83952 | C30 | 0.4259 | 0.45093 | 0.3131 |
| C13 | 0.48641 | 0.45341 | 0.34175 | C31 | 0.35935 | 0.56256 | 0.46901 |
| C14 | 0.36907 | 0.39022 | 0.2547 | C32 | 0.42174 | 0.51122 | 0.35136 |
| C15 | 0.37243 | 0.33264 | 0.22458 | C33 | 0.47279 | 0.62711 | 0.35496 |
| C16 | 0.29252 | 0.6137 | 0.64971 | C34 | 0.70972 | 0.76088 | 0.03618 |
| C17 | 0.2322 | 0.60886 | 0.72804 | C35 | 0.75112 | 0.88055 | -0.06211 |
| C18 | 0.17412 | 0.54703 | 0.71039 | C36 | 0.23 | 0.66984 | 0.82665 |

**Continuous Table S1.** Fractional atomic coordinates for the unit cell of CBF with AA-stacking.

| Atom | *x/a* | *y/b* | *z/c* | Atom | *x/a* | *y/b* | *z/c* |
|---|---|---|---|---|---|---|---|
| C37 | 0.11336 | 0.59101 | 0.9952 | C60 | -1.87592 | 3.97117 | 1.84991 |
| C38 | 0.19465 | 0.77334 | 0.82962 | H61 | 0.53289 | 0.5028 | 0.38739 |
| C39 | 0.17811 | 0.82268 | 0.79871 | H62 | 0.31955 | 0.38754 | 0.23139 |
| C40 | 0.11272 | 0.80619 | 0.74654 | H63 | 0.33922 | 0.66376 | 0.66491 |
| C41 | 0.06418 | 0.73968 | 0.72396 | H64 | 0.13086 | 0.44138 | 0.58964 |
| C42 | 0.08062 | 0.69036 | 0.75781 | H65 | 0.24051 | 0.45071 | 0.45583 |
| C43 | 0.14597 | 0.70668 | 0.81208 | H66 | 0.5938 | 0.64976 | 0.1552 |
| C44 | 0.17609 | 0.03283 | 0.66822 | H67 | 0.58246 | 0.85809 | 0.35332 |
| C45 | 0.23556 | 0.03929 | 0.54647 | H68 | 0.48129 | 0.74655 | 0.44564 |
| C46 | 0.28393 | 0.09875 | 0.3959 | H69 | 0.5393 | 0.39813 | 0.34222 |
| C47 | 0.27369 | 0.15264 | 0.36501 | H70 | 0.70488 | 0.74173 | -0.25489 |
| C48 | 0.21433 | 0.14594 | 0.48901 | H71 | 0.72017 | 0.72897 | 0.22834 |
| C49 | 0.16624 | 0.0868 | 0.64041 | H72 | 0.73635 | 0.87323 | -0.36231 |
| C50 | 0.842 | 0.79325 | 0.25059 | H73 | 0.79729 | 0.93053 | -0.0254 |
| C51 | 0.90385 | 0.80811 | 0.37768 | H74 | 0.25598 | 0.70865 | 0.60584 |
| C52 | 0.95189 | 0.87356 | 0.44725 | H75 | 0.25598 | 0.68975 | 1.09871 |
| C53 | 0.93729 | 0.92385 | 0.38646 | H76 | 0.06301 | 0.58675 | 0.98773 |
| C54 | 0.87567 | 0.90905 | 0.25794 | H77 | 0.12561 | 0.58477 | 1.28837 |
| C55 | 0.82734 | 0.84361 | 0.18913 | H78 | 0.24812 | 0.78756 | 0.86934 |
| C56 | 0.3108 | 0.26873 | 0.16124 | H79 | 0.21792 | 0.87671 | 0.81591 |
| C57 | 0.38467 | 0.22233 | 0.06844 | H80 | 0.01088 | 0.72555 | 0.67769 |
| C58 | -2.98306 | 2.88978 | 0.58586 | H81 | 0.04079 | 0.63634 | 0.7414 |
| C59 | -1.90518 | 3.858 | 1.72634 | H82 | 0.24458 | -0.00403 | 0.57012 |

**Continuous Table S1.** Fractional atomic coordinates for the unit cell of CBF with AA-stacking.

| Atom | *x/a* | *y/b* | *z/c* | Atom | *x/a* | *y/b* | *z/c* |
|---|---|---|---|---|---|---|---|
| H83 | 0.33208 | 0.10369 | 0.29722 | H90 | 0.29228 | 0.26815 | -0.12706 |
| H84 | 0.20506 | 0.18911 | 0.46645 | H91 | 0.27204 | 0.26319 | 0.36685 |
| H85 | 0.11857 | 0.08261 | 0.74203 | H92 | 0.38747 | 0.23042 | -0.23948 |
| H86 | 0.80332 | 0.73974 | 0.19681 | H93 | 0.38782 | 0.17636 | 0.13116 |
| H87 | 0.91537 | 0.7669 | 0.42515 | H94 | -1.87684 | 3.98367 | 2.14988 |
| H88 | 0.97589 | 0.97732 | 0.44206 | H95 | -1.95457 | 3.9905 | 1.6818 |
| H89 | 0.8643 | 0.95031 | 0.20805 | | | | |

**Table S2.** Comparison of N-DMC with other polybenzoxazine to porous carbons for $CO_2$ uptake

| Materials | Adsorption at 0 °C (mmol $g^{-1}$ ) | Adsorption at 25 °C (mmol $g^{-1}$ ) | Surface area ($m^2$ $g^{-1}$) | Ref. |
|---|---|---|---|---|
| Soft template F127 followed by KOH | 4.36 | 3.21 | 1188 | S1 |
| Soft template F127 | 6.35 | 4.02 | 1257 | S2 |
| Soft-templating and KOH chemical activation | 6.20 | 3.95 | 2267 | S3 |
| Hydrothermal synthesis in resorcinol/ formaldehyde and ethylenediamine (EDA) | 6.20 | 4.10 | 1224 | S4 |
| N-DMC | 7.46 | 3.85 | 1469 | This work |

**Table S3.** Comparison between specific capacitance of N-DMC with those of previously reported N-doped porous carbons for supercapacitor application.

| Materials | Surface area ($m^2$ $g^{-1}$) | Capacitance | Ref |
|---|---|---|---|
| N- doped carbos | 1256 | 261 F $g^{-1}$@ 0.05 A $g^{-1}$ | S5 |
| Asphaltene-based porous carbon | 2168 | 135.4 $Fg^{-1}$ @ 1 $Ag^{-1}$ | S6 |
| Heating exfoliated GIC at 2000 °C | 50 | 90 $Fg^{-1}$ @ 5$mVs^{-1}$ | S7 |
| Pyrolysis of pistachio nutshell | 1900 | 45 $Fg^{-1}$ @ 1 $mVs^{-1}$ | S8 |
| Hollow carbon-$MoS_2$-carbon nanoplates | 543 | 178 $Fg^{-1}$ @ 1.0 $Ag^{-1}$ | S9 |
| Activated carbon fiber yarns | 1600 | 45.2 mF $cm^{-1}$@ 2 $mVs^{-1}$ | S10 |
| Mesoporous nitrogen-doped hollow carbon nanoplates with uniform hexagonal morphologies | 460 | 95 $Fg^{-1}$ @ 1.0 $Ag^{-1}$ | S11 |
| Carbon nanotube composite with activated carbon | - | 60.75 F $cm^{-3}$ | S12 |
| Nanoholes on single-walled carbon nanohorn | 1020 | 8.6 µF $cm^{-2}$ | S13 |
| Tnnic acid and carbon nanotubes | - | 147.4 $Fg^{-1}$@ 0.5 $Ag^{-1}$ | S14 |
| Carbon composite and replica | 1535 | 92.6 µF$cm^{-2}$ | S15 |
| Carbons derived from Peach Gum | 95 | 199 $Fg^{-1}$ @ 0.2 $Ag^{-1}$ | S16 |
| N- doped Porous carbons ropes | 300 | 60 $Fg^{-1}$@ 1.0 $Ag^{-1}$ | S17 |
| Carbonization of poly(benzoxazine-*co*-resol) | 376 | 247 $Fg^{-1}$@ 0.5 $Ag^{-1}$ | S18 |
| N-DMC | 1469 | 185 $Fg^{-1}$@ 1.0 $Ag^{-1}$ | This work |

## References


S1. S. Wang, W. C. Li, L. Zhang, Z. Y. Jin, and A. H. Lu, *J. Mater. Chem. A*, 2014, **2**, 4406-4412.

S2. L. Wan, J. Wang, C. Feng, Y. Sun, and K. Li, *Nanoscale,* 2015, **7**, 6534-6544.

S3. L. Wan, J. Wang, Y. Sun, C. Feng, and K. Li, *RSC Adv.*, 2015**, 5**, 5331-5342.

S4. N. P. Wickramaratne, J. Xu, M. Wang, L. Zhu, L. Dai, and M. Jaroniec, *Chem. Mater.*, 2014, **26**, 2820-2828.

S5. J. Zhang, W. Zhang, M. Han, and J. Pang, *J. Mater. Sci.: Mater. in Electron.*, 2018**, 29**, 4639-4648.

S6. F. Qin, X. Tian, Z. Guo, and W. Shen, *ACS Sus. Chem. Eng.,* 2018**, 6**, 15708-15719.

S7. B. H. Wee, T. F. Wu, and J. D. Hong, *ACS App. Mater. Int.*, 2017**, 9**, 4548-4557.

S8. J. L. Goldfarb, G. Dou, M. Salari, and M. W. Grinstaff, *ACS Sus. Chem. Eng.*, 2017**, 5**, 3046-3054.

S9. T. Quan, N. Goubard-Bretesché, E. Härk, Z. Kochovski, S. Mei, N. Pinna, M. Ballauff, and Y. Lu, *Chem. Eur. J.,* 2019**, 25**, 4757-4766.

S10. S. Zhai, W. Jiang, L. Wei, H. E. Karahan, Y. Yuan, A. K Ng, and Y. Chen, *Mater. Horizons*, 2015**, 2**, 598-605.

S11. J. Cao, C. J. Jafta, J. Gong, Q. Ran, X. Lin, R. Félix, R. G. Wilks, M. Bär,; J. Yuan,; M. Ballauff, and Y. Lu, *ACS App. Mater. Int.*, 2016**, 8**, 29628-29636.

S12. H. Park, R. B. Ambade, S. H. Noh, W. Eom, K. H. Koh, S. B. Ambade, W. J. Lee, S. H. Kim, and T. H. Han, *ACS App.Mater.Int.,* 2019**, 11**, 9011-9022.

S13. C.-M. Yang, Y.-J. Kim, J. Miyawaki, Y. A. Kim, M. Yudasaka, S. Iijima, and K. Kaneko, *J. Phys. Chem. C*, 2015**, 119**, 2935-2940.

S14. J. Y. Oh, Y. Jung, Y. S. Cho, J. Choi, J. H. Youk, N. Fechler, S. J. Yang, and C. R. Park, *ChemSusChem.,* 2017**, 10**, 1675-1682.

S15. T. Stimpfling, and F. Leroux, *Chem. Mater.*, 2010**, 22**, 974-987.

S16. Y. Lin, Z. Chen, C. Yu, and W. Zhong, *ACS Sus. Chem. Eng.* 2019**, 7**, 3389-3403.

S17. P. Thirukumaran, A. Parven, Y. R. Lee, and S. C. Kim, *J. Alloys Comp.,* 2018**, 750,** 384-391.

S18. D.-C. Guo, J. Mi, G.-P. Hao, W. Dong, G. Xiong, W.-C. Li, and A.-H. Lu, *Energy Environ. Sci.,* 2013**, 6,** 652-659.